SOLID PARTICLE EROSION RESISTANCE AND HIGH STRAIN RATE DEFORMATION BEHAVIOR OF INCONEL-625 ALLOY

B.F. Levin, K.S. Vecchio*, J.N. DuPont, and A.R. Marder
Lehigh University, Energy Research Center, Bethlehem, PA 18015
*University of California at San Diego, Department of Applied Mechanics and Engineering Sciences, La Jolla, CA 92093

Abstract

The room temperature erosion behavior and high strain rate deformation behavior of wrought Inconel-625 alloy was evaluated. To determine erosion resistance, the steady state erosion rate was measured. Microhardness tests were performed after the erosion tests and significant plastic deformation was observed in the vicinity of the eroded surfaces. To investigate the effect of mechanical properties on erosion resistance, compression tests were conducted at high strain rates (1700-9000s^{-1}) that are comparable to strain rates during erosion. High strain rate compression tests were also conducted at elevated temperatures (400^{0}C and 600^{0}C) to observe the combined effect of strain rate and temperature on mechanical properties. Microhardness at the eroded surfaces and high strain rate toughness were correlated to the erosion resistance. The relationships between toughness, high strain rate mechanical properties, and erosion resistance are discussed. The erosion resistance of Inconel-625 is compared with erosion resistance of other Ni and Fe-based alloys.

I. Introduction

Solid Particle Erosion (SPE) is a loss of material during repetitive impacts of solid particles and one of the primary reasons for the damage of power generation components. More than 25% of all boiler tube failures are caused by solid particle erosion [1] and, therefore, the design and proper selection of erosion resistant materials can significantly reduce the operating costs of power generation. Many attempts have been made to correlate erosion resistance to readily measurable mechanical properties. Some of these properties include hardness, ductility, yield and fatigue strength, and the strain hardening coefficient [2,3]. However, no simple correlation to predict erosion resistance using a single property or combination of properties has been developed. The lack of a relationship between mechanical properties and erosion resistance can be attributed to the difference in strain rates during erosion and conventional mechanical tests. Typically, strain rates during SPE range from 10^3 to10^6 s^{-1}, while strain rates during quasi-static mechanical tests (i.e., tensile or hardness tests) vary from 10^{-4} to10^{-2} s^{-1} [4]. Since SPE involves high strain rate deformation of a target material, its erosion resistance may be related to the high strain rate mechanical properties. Because Inconel-625 alloy is often used in power generation components, it is the purpose of this research to investigate the erosion behavior and *high strain rate* mechanical properties of this alloy and compare it with other commercially available alloys.

Superalloys 718, 625, 706 and Various Derivatives
Edited by E.A. Loria
The Minerals, Metals & Materials Society, 1997

II. Experimental Procedure

II. A. Erosion Tests

The erosion tester used in this study is described elsewhere [5] and the standard test conditions are presented in Table I. Seven different erosion exposure times (30-210min.) were used to adequately obtain the weight loss vs. time plot, the slope of which yielded the steady state erosion rate. To quantify weight loss during the erosion experiments, the erosion specimens were ultrasonically cleaned in acetone and weighed before and after the erosion tests to the nearest 0.1 mg. The volumetric erosion rate was obtained by dividing the weight loss rate by the density of the alloy.

Table I. Erosion tests conditions.

Eroded Sample Planar Dimensions	1.3 cm x 1.3 cm
Sample Temperature	20°C
Erodent Particle Velocity	40 m/s ±5 m/s
Erodent Particles Flux	8.6 mg/(mm2/sec)
Impingement Angle	90°
Erodent	angular alumina (Al2O3)
Erodent Size Range	300-425 μm.
Average Diameter Of The Erodent	350 μm

II.B. Mechanical Tests

To determine the size of the deformed region beneath the eroded surface and maximum hardness at the eroded surface, microhardness tests were performed on a cross-section of Inconel-625 after the longest exposure time of 210 min. Because of erosion, the material beneath the eroded surface may experience plastic deformation that results in an increase in hardness below the surface. The depth of plastic deformation can be estimated by obtaining a microhardness profile from the eroded surface into the base material. A schematic diagram of this profile is shown in Figure 1. The depth at which the hardness value becomes constant is defined as the plastic zone size. All measurements were performed using a Knoop indenter with a test load of 10g. The Knoop indenter minimizes the specimen edge effect on microhardness results, allowing the tests to begin at 5-10 μm from the eroded surface. Three to five profiles were obtained in different locations in order to improve the statistical significance of the data.

Compression tests in the quasi-static regime were conducted on a conventional servo-hydraulic test frame, and tests in the high strain-rate regime were conducted using a compression split-Hopkinson pressure bar. Strain rates during the tests varied between 2000 s^{-1} and 9000 s^{-1} and are similar to those calculated by Hutchings [6] during particle impacts at 40 m/s. Therefore, the mechanical properties measured from the high strain rate tests can be used as an estimate of the mechanical properties of the target material during erosion. Compression specimens were machined as right, regular cylinders with a diameter and height of 5.1 mm. For the elevated temperature tests conducted at high strain rates, the specimens were heated by a small tube furnace attached to the split-Hopkinson bar apparatus, with the specimens suspended within the furnace by a thermocouple wire wrapped around the sample. This thermocouple was also used to monitor the specimen temperature during heating. The incident and transmission bars are held outside the furnace during the initial heating of the specimen and are mechanically slid into the furnace to lightly contact the specimen a few microseconds before the incident stress pulse impacts the sample.

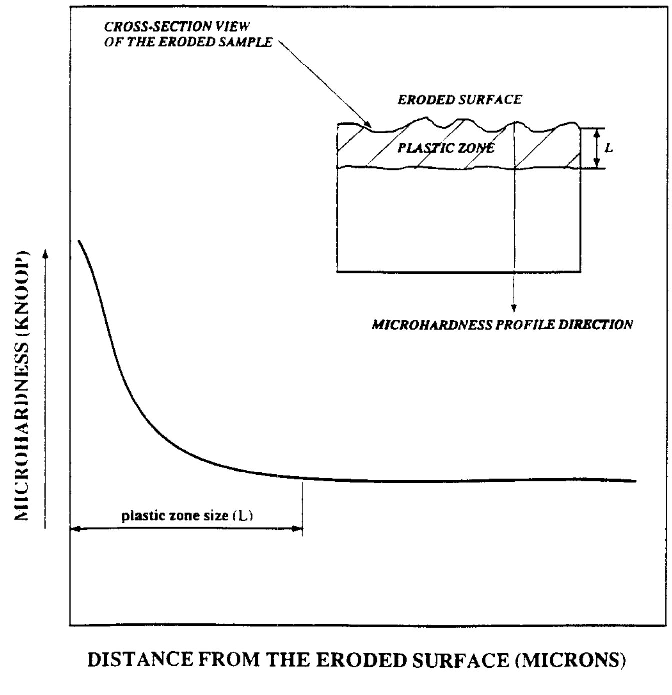

Figure 1. Schematic diagram of the microhardness technique that was used to measure plastic deformation below the eroded surface.

III. Results and Discussion

III.A. Erosion Tests and Plastic Deformation During Erosion

A weight loss versus time plot for the Inconel-625 alloy is presented in Figure 2. The weight loss and volume loss rates were determined to be 0.127 mg/min and 0.015 mm^3/min, respectively. Results of the microhardness tests (Figure 3) showed a significant increase in hardness near the eroded surface and presence of the plastically deformed region ($\approx 50\ \mu m$) beneath the eroded surface. Plastic deformation during erosion suggests that erosion resistance of Inconel-625 should be related to its ability to *absorb* impact energy. Mechanical properties such as hardness and toughness affect a material's ability to deform plastically and may control its erosion resistance.

Figure 4 shows the stress-strain behavior for Inconel-625 over a wide range of strain rates and temperatures. The flow stress and strain hardening rate of the material increase with increasing strain rate or decreasing temperature. The significant increase in initial yield strength with increasing strain rate is in contrast to the behavior of pure FCC metals which typically show little or no influence of strain rate on yield strength. The relatively high strain rate and temperature sensitivity displayed by Inconel 625 demonstrates the importance of conducting high strain rate tests when attempting to develop correlations between erosion (a high strain rate deformation process) and mechanical properties. The effect of high strain rate mechanical properties on erosion resistance can be analyzed based on the energy balance during particle impact.

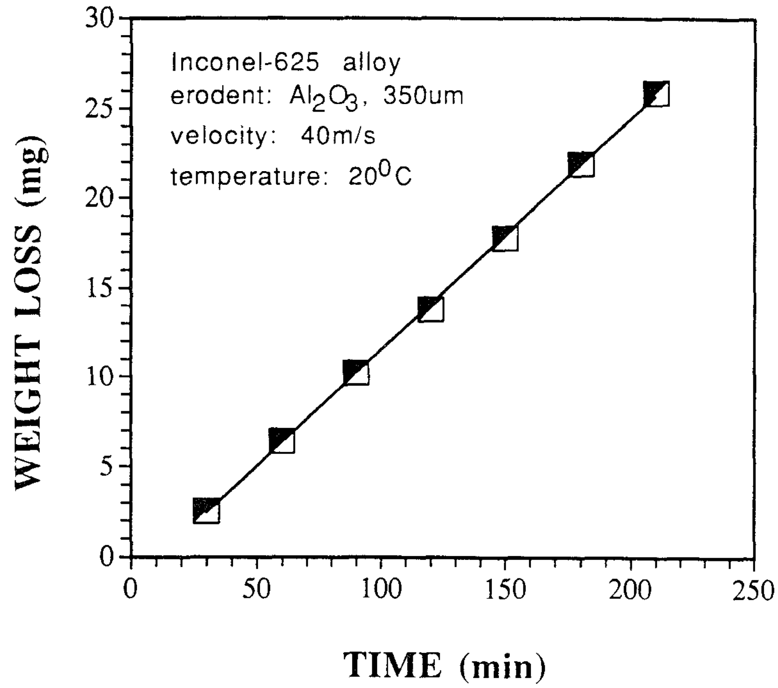

Figure 2. Weight loss versus erosion time plot for the Inconel-625 alloy. The slope of this represents steady state erosion rate.

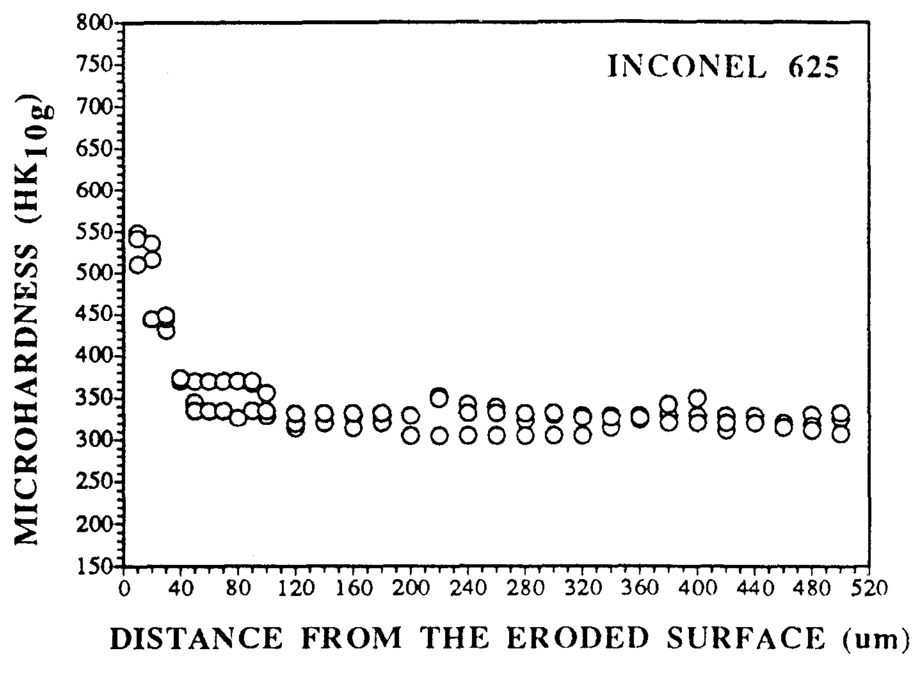

Figure 3. Microhardness profiles obtained on the cross-sections of the eroded samples after the longest exposure time (210 min).

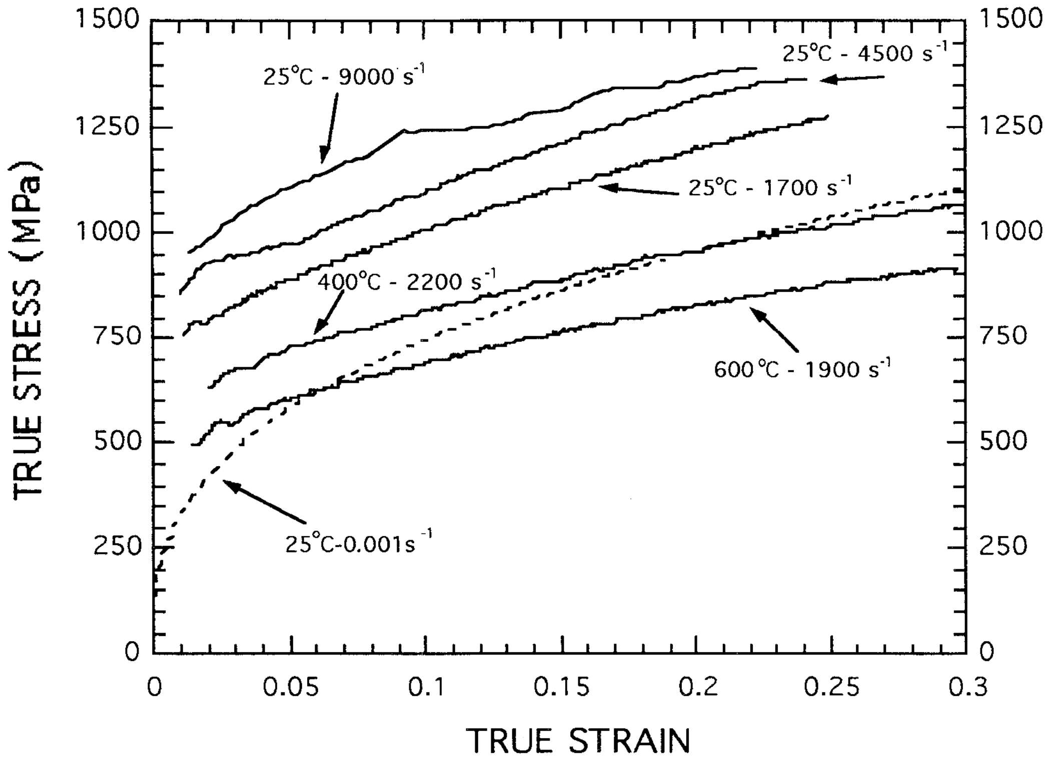

Figure 4. Quasi-static and high-strain rate compression stress-strain curves for the Inconel-625.

III.B. Effect of Mechanical Properties on Energy Dissipation During Erosion

To consider the effect of target material mechanical properties on erosion resistance, the following assumptions can be made to simplify the energy balance between an impacting particle and target material: 1) the erodent particle is spherical and does not brake upon impact and 2) the amount of kinetic energy converted to heat during impact is negligible.

III.B.1. Plastic Deformation Energy The kinetic energy of the particle before the impact is given by:

$$KE = \frac{m V_i^2}{2} \qquad (1)$$

where m is the mass of the particle and V_i is initial velocity. The portion of the initial kinetic energy used for plastic deformation (KE_{pd}) is equal to:

$$KE_{pd} = \frac{m V_i^2}{2} - \frac{m V_r^2}{2} = \frac{m V_i^2}{2} [1 - (\frac{V_r}{V_i})^2] \qquad (2)$$

where V_r is the rebound velocity of the particle. The term V_r/V_i, the coefficient of restitution (e), represents the stored elastic energy in the particle and the target material after the impact. The coefficient of restitution depends on the mechanical properties of the particle and target materials (i.e., hardness and elastic modulus).

According to Lankov [7] and Johnson [8], the coefficient of restitution for spherical particles can be expressed as a function of hardness and elastic modulus:

$$e = \left(\frac{V_r}{V_i}\right) = \frac{(1.8\ H^{5/8}\ J^{1/2})}{(\rho_p^{1/8}\ V_i^{1/4})} \tag{3}$$

or

$$e^2 = \left(\frac{V_r}{V_i}\right)^2 = \frac{(3.1\ H^{5/4}\ J)}{(\rho_p^{1/4}\ V_i^{1/2})} \tag{4}$$

where, ρ_p is the density of the impacting spherical particle in kg/m^3, H is the target material hardness in N/m^2, V_i is the initial particle velocity in m/s, and J is a parameter related to the elastic modulus and Poisson coefficient of the target and particle materials:

$$J = \frac{(1 - \mu_t^2)}{E_t} + \frac{(1 - \mu_p^2)}{E_p} \tag{5}$$

where μ_t and μ_p are the Poisson coefficients of the target and particle materials respectively, and E_t and E_p are the elastic modulus of the target and particle material, respectively in N/m^2. Substitution of the experimental values used in this study for the velocity of the erodent and mechanical properties of the Inconel-625 and erodent in eq. 4 and 5 (V_i = 40 m/s, E_t =210*10^9 N/m^2, E_p = 400*10^9 N/m^2, μ_p= 0, μ_t = 0.35, and ρ_p = 4000 kg/m^3), will give an expression for the coefficient of restitution as a function of material hardness:

$$e^2 = 0.41\ x\ 10^{-12}\ H^{\frac{5}{4}} \tag{6}$$

Therefore, equation 2 can be written as:

$$KE_{pd} \cong \frac{mV_i^2}{2}\left(1 - 0.41\ x\ 10^{-12}\ H^{\frac{5}{4}}\right) \tag{7}$$

Equation 7 shows that, for target material with high hardness, a larger portion of the particle kinetic energy transforms into rebound when compared with materials with low hardness.

III.B.2. Erosion Parameter Bitter [9] suggested that the erosion rate is proportional to the ratio of the input kinetic energy to the energy needed to remove a unit volume of the material. Thus, the erosion rate of the material will be determined by the ratio of the energy used for plastic deformation, KE_{pd}, to the energy per unit volume required to *cause fracture* (i.e., the fracture energy). The fracture energy per unit volume can be represented by the toughness, which is given simply by the area under the stress-strain curve. Now the expression for an erosion parameter can be written as follows:

$$E \sim \frac{KE_{pd}}{T} \sim \frac{mV_i^2\ (1-e^2)}{2\ T} \qquad (8)$$

where E is the erosion parameter and T is the tensile toughness of the target material. Using equation 7 for KE_{pd}, equation 8 can be rewritten to give an expression for the erosion parameter in terms of hardness and toughness of the target material:

$$E \sim \frac{mV_i^2}{2} \frac{(1 - 0.41\ x\ 10^{-12}\ H^{\frac{5}{4}})}{T} \qquad (9)$$

This expression shows that the erosion parameter is low (erosion resistance is high) for materials that combine high hardness and toughness. To evaluate the validity of equation 9, the toughness of Inconel 625 and several other austentic alloys was estimated from high strain rate compression tests. Also, the maximum hardness beneath the eroded surface was substituted as H in equation 9. The procedure for the estimate of the mechanical properties during erosion is presented below.

III.C. Mechanical Properties During Erosion

To estimate the tensile toughness (T) of Inconel-625 during erosion, the following procedures were conducted: 1) compression stress-strain curves at strain rates comparable to those during erosion were generated, 2) stress and strain to failure at the eroded surface were estimated, and 3) toughness was found by integration of the compression stress-strain curves over the strain range from zero to the failure strain.

III.C.1. Estimation of Tensile Toughness During Erosion For eroded materials, failure strength can be estimated from the microhardness profiles beneath the eroded surface. During particle impact, the yield strength of the material is locally exceeded and plastic deformation takes place in the vicinity of the impact. Upon further deformation, the yield strength at the surface of the material will eventually become equal to its fracture strength. Thus, the hardness at the eroded surface may be used to estimate fracture strength. The relationship between hardness and strength can be written as [10]:

$$H = A\ \sigma_f \qquad (10)$$

where H is the hardness, σ_f is the flow stress, and A is a constant.

To determine the hardness at the eroded surface, 10g Knoop microhardness tests were conducted on both high strain rate compression samples and cross-sectional erosion samples. Using known stress values from the high strain rate compression curves (Figure 4) and corresponding hardness values, the constant A was determined using equation 10. Subsequently, the value of A was used to calculate the failure strength from the microhardness measurements near the eroded surface (5μm from the surface). Results of the hardness-stress conversion are shown in Table II. Once the fracture strength was determined, the fracture strain and toughness were found from the room temperature high strain rate compression stress-strain curves. A schematic illustration of this procedure is shown in Figure 5. The estimated failure strength, failure strain, and tensile toughness values for Inconel 625 are listed in Table III. Tensile toughness (T) and the maximum hardness near the eroded surface (H) can be used to examine the validity of equation 9 for the erosion parameter and determine the combined effects of hardness and toughness on erosion resistance.

Table II. Hardness-strength conversion ($H=A\sigma$ [10]).

Alloy	Strain rate (s^{-1})	Stress, σ (MPa)	Hardness, H (10g Knoop) (MPa)	Constant, $A=H/\sigma$ (average value)	Hardness at the eroded surface (10g, Knoop) (MPa)	Failure strength at the eroded surface (MPa)
IN-625	1700 4500 9000	1250 1350 1400	4410±530 4580±220 4740±260	3.5	5340±210	1526±60

[1]Hardness numbers and standard deviations were calculated from at least 10-20 indentations.

Table III. Estimated failure strength, failure strain, and tensile toughness values during erosion.

Alloy	Strain rate, (s^{-1})	Failure strength (MPa)	Failure strain	Toughness (Mjoules/m^3)
IN-625	9000	1526±60	0.24±0.02	295±32

III.C.3. Effect of Mechanical Properties on Erosion Resistance The calculated erosion parameter, E, from equation 9 is plotted against experimentally determined volumetric erosion rates for the Inconel-625 and other nickel, cobalt, and iron based superalloys in Figure 6. It can be seen that a decrease in the value of E leads to a decrease in erosion rate. These results show that materials combining high hardness and toughness at high strain rates (Ultimet, Inconel-625, Hastelloy C-22) have low values of E and therefore, provide good erosion resistance. Hardness is necessary to reduce the energy transferred from the particle into the material and toughness is indicative of the material's ability to absorb this energy without fracture. However, high hardness may reduce the material's ability to deform plastically and therefore, its toughness may decrease. The optimum combination of these properties provides the best erosion resistance.

If a ductile material is not strain rate sensitive, its quasi-static mechanical properties can be used for approximate correlations to erosion resistance. However, for most ductile materials, the mechanical properties measured at high strain rates are different from the quasi-static properties. Since SPE involves high strain rate deformation of the target material, caution must be taken when the relationships between quasi-static mechanical properties and erosion resistance are drawn. Unfortunately, the exact strain rates during erosion are difficult to estimate because of the gradual change in mechanical properties with distance from the eroded surface. However, high strain rate compression tests along with microhardness measurements can provide a reasonable estimate of the mechanical properties during erosion and should be used to predict erosion behavior of materials.

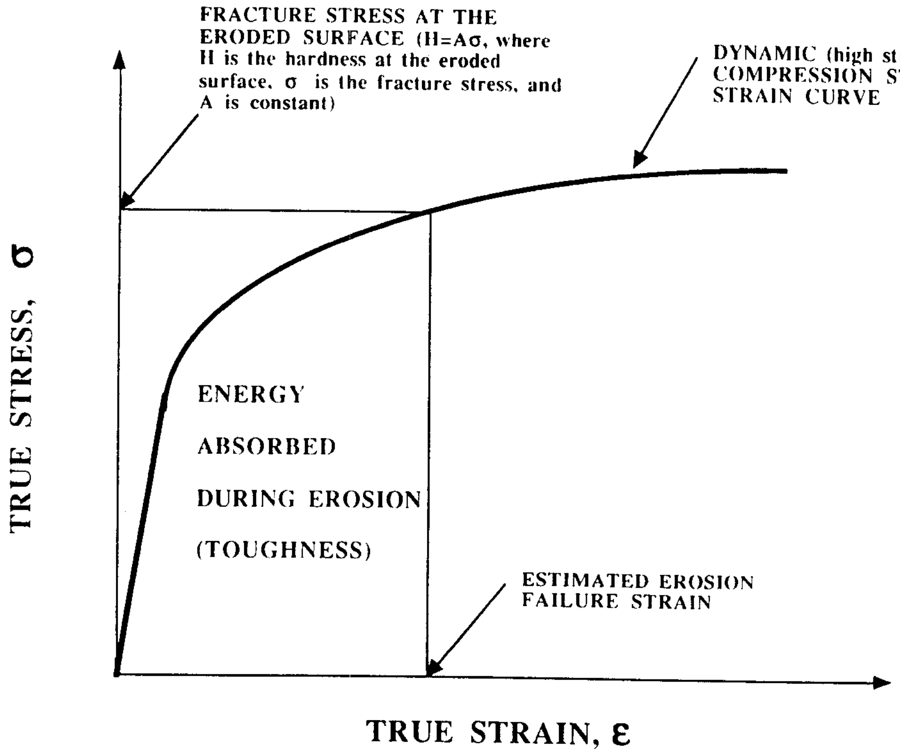

Figure 5. Schematic diagram showing procedure that was used to estimate tensile toughness during erosion using high strain rate compression and microhardness tests.

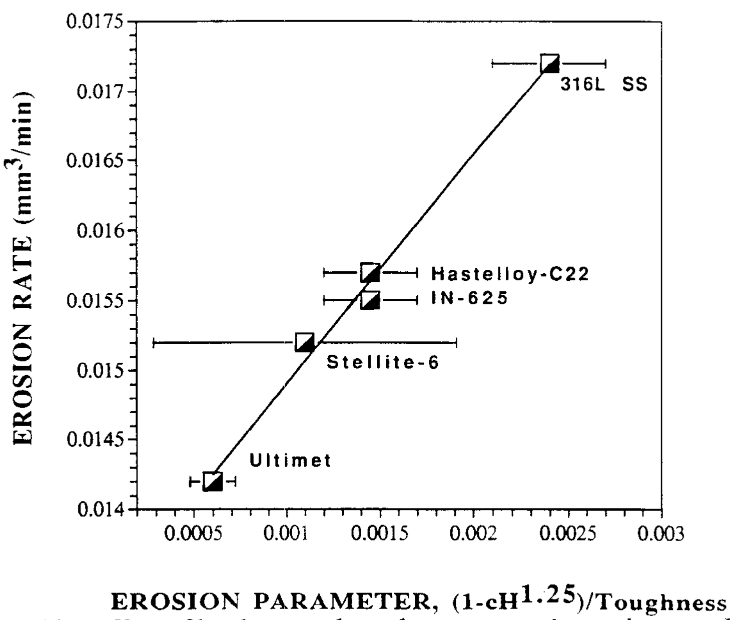

Figure 6. The combine effect of hardness and toughness on erosion resistance. Erosion parameter calculated from equation 11 is plotted against experimentally determined

IV. Conclusions

Erosion and deformation behavior of wrought Inconel-625 were analyzed and compared with other commercially available Ni, Co, and Fe-base alloys. High strain rate mechanical tests along with microhardness tests were used to estimate mechanical properties during erosion. Based on the results of this study, the following can be concluded:

1. Inconel-625 showed significant strain rate and temperature sensitivity. The flow stress and strain hardening rate of the material increases with increasing strain rate or decreasing temperature

2. A procedure for estimating mechanical properties during erosion using high strain rate compression tests and microhardness measurements was developed. Based on energy balance considerations, an erosion parameter was propsed which showed good correlation with experimentally measured erosion rates for several alloys.

3. Alloys that combine high hardness and toughness at high strain rates (Inconel-625, Ultimet, and Hastelloy-C22) showed good erosion resistance at room temperature. Hardness is necessary to reduce energy transferred from the particle into the material while toughness is indicative of the material's ability to absorb this energy without fracture.

V. References

1. Stringer, J., Wear, 186-187, 1995, p.11.
2. Meng, H.C. and Ludema, K.C., *Wear*, 181-183, 1995, p. 443.
3. Richman, R.H. and McNaughton, W.P., *Wear*, 140, 1990, p. 63.
4. Sundararajan, G., *Wear,* 186-187, 1995, p. 129.
5. Lindsley, B., Stein, K., and Marder, A.R., *Measurement Science Technology*, 6, 1995, p. 1169.
6. Hutchings, I.M., *J. Phys. D: Appl.Phys.*, Vol.10, 1977, p. L179.
7. Lankov, A. A., *Trenie and Iznos* (Russian), 13, n.1, 1992, p. 206.
8. Johnson, K.L. Contact Mechanics, Cambridge University Press, 1985, p. 363
9. Bitter, J.G.A., *Wear*, 6, 1963, p. 5.
10. Tabor, D., The Hardness of Metals, Clarendon Press, Oxford, 1951.